Autonomous Robots 18, 5–20, 2005

Control of a Robotic Wheelchair Using Recurrent Networks

LUCIANO BOQUETE, RAFAEL BAREA, RICARDO GARCÍA, MANUEL MAZO
AND M. ANGEL SOTELO
Electronics Department, Alcalá University, 28801 Spain
luciano@depeca.uah.es
luciano.boquete@uah.es

Abstract. This paper describes an adaptive neural control system for governing the movements of a robotic wheelchair. It presents a new model of recurrent neural network based on a RBF architecture and combining in its architecture local recurrence and synaptic connections with FIR filters. This model is used in two different control architectures to command the movements of a robotic wheelchair. The training equations and the stability conditions of the control system are obtained. Practical tests show that the results achieved using the proposed method are better than those obtained using PID controllers or other recurrent neural networks models

Keywords: neurocontrol, recurrent neural networks, radial basis function, dynamics, identification, stability, adaptive control

1. Introduction

In recent years there has been an outstanding in the applications of neural networks, due to their ability to learn from examples and approximate any non-linear function. The most successful topologies are the multilayer perceptron (MLP) and radial basis function (RBF) networks (Mulgrew, 1996). Both models can approximate any continuous non-linear function, although the MLP model suffers from the drawback of being slow to train, due to the need to backpropagate the error; this handicap makes it impossible to use in many practical applications. RBF networks were initially developed for the interpolation of data in multidimensional spaces. The advantages of these networks are their simplicity and their trainability by means of easy to implement algorithms with a high convergence speed, as there is a linear relationship between the parameters to be adjusted (synaptic connections) and the neural network output (Chen et al., 1993).

Both types of neural topologies can be classified into feed-forward models and recurrent models. In the latter there is some sort of feedback loop in their structure, or inputs at different moments of time are considered, so that the neural network output depends on the past history of the network.

When implementing a recurrent neural network the difference between the various architectures resides on how the network feedback is carried out (Campolucci et al., 1999): either externally or internally. Examples of external feedback are the Tapped Delay Line networks, the model of Narendra and Parthasarathy (NARX neural network) (Narendra and Parthasarathy, 1990) or the Elman's networks (Elman, 1990). As for internal feedback, there are several possibilities, such as neural networks totally connected up to each other (globally recurrent neural networks), using a FIR/IIR filter as synaptic connections (Figueiredo, 1998; Ciocoiu, 1996), storage units (Sastry et al., 1994), etc.

This paper presents a new model of RBF-type network with FIR filters between the output of each neuron and each input of the same neuron; it also uses an FIR filter as synaptic connection between each neuron and the output of the neural network. As a practical test of its behaviour, the model described is used for implementing the adaptive controller of a robotic wheelchair navigator.

The robotic wheelchair is guided by using an inverse control system, where the neurocontroller generates the

control signals that ensure the output of the controlled plant is the appropriate one. When using an inverse control system, in which the controller is a neural network, the problem is how to propagate the control error to the adjustable coefficients of the neurocontroller in such a way that the latter vary in the right direction, leading to error reduction. In short, the problem is how to obtain the sensitivity of each plant output with respect to each input.

One possibility involves obtaining a behaviour model of the plant to be controlled, and then obtaining from such mathematical model the necessary data for adjusting the controller. This problem has been solved in different ways: thus, Ku and Lee (1995) and Zhang et al. (1995) use a neuroidentifier in parallel with the physical system to be controlled. This neuroidentifier, which may be a recurrent neural network or a feed-forward network with inputs at different moments of time, serves as an error propagation path. Zhang et al. (1995) use only the sign or direction of variation produced on an output by an input change, as this information suffices for assessing in which direction each of the neurocontroller coefficients have to be adjusted; Acosta et al. (1999) calculate this sensitivity by finding the relation between the plant's output at two different instants of time and the variation in the input that has produced said variation, i.e.:

$$\frac{\partial y(k)}{\partial u(k)} \simeq \frac{y(k) - y(k-1)}{u(k) - u(k-1)} \tag{1}$$

Another possibility is that used by Maeda and Figueiredo (1997), who obtain said sensitivity by increasing each one of the neurocontroller's adjustable coefficients and making the corresponding observation of the variations in each of the plant outputs to be controlled, thereby estimating the plant Jacobian.

This paper presents two different possibilities; the first one is based on the possibility of obtaining an approximation of the dynamic behaviour of the wheelchair, from which its Jacobian can be calculated, along the same lines as the system used by Zhang et al. (1995) for controlling a ship; the second option involves using another neural network in parallel with the robotic wheelchair, acting as neuroidentifier, thus serving as a path for propagating the control error through the wheelchair's dynamic, providing that the identification error is negligible.

1.1. Control of Robotic Wheelchairs

The development of robotic systems for aiding elderly and/or disabled persons is motivated by two factors: firstly, the increase in the number of people needing this assistance and secondly the ongoing technical breakthroughs that make the robotic systems themselves more efficient. From the mechanical point of view the models include the following possibilities: classic wheelchairs for disabled people (Mazo et al., 2001; Cooper et al., 2002), systems for going up and down stairs like INDEPEND ENCE™ iBOT™ 3000 Mobility System, systems with legs for overcoming certain obstacles (Wellman et al., 1995; Krovi and Kumar, 1999) or canes or walkers as mobility aids for people who are able to walk (Yu et al., 2003), among other possibilities.

In this paper a conventional wheelchair is used (Fig. 1) and the aim in view is to design a wheelchair control system that works better than the basic PID system incorporated therein. The working conditions of a robotic wheelchair vary greatly and these variations entail changes in its dynamic model. In order to

Figure 1. Actual image of the wheelchair.

ilustrate the previous statement the following effects can be mentioned:

- differences in the weight of the various users; the dynamics of the wheelchair are quite different when the driver is a child as compared to an adult (Brown et al., 1990),
- movements of the user in the wheelchair, involving a displacement of the mass centre,
- variations in the friction between wheels and the ground and wheel skidding,
- ground gradient variations,
- existence of backslash in the MOSFET based H bridge response (Cooper, 1995),
- functional asymmetries or differences in the various motors and their associated mechanics,
- other effects such as variations in the battery charging level, ageing of elements, etc.

The variation of parameter in the wheelchair application are therefore a significant problem (Brown et al., 1990). These systems are so complex, therefore, that is impractical to describe the dynamics by exact mathematical models (Cooper, 1995). As a result, it is difficult to solve the inverse kinematics of the system for obtaining the desired actuator velocity.

In general the speed control system of a mobile robot can be structured on several levels:

- low-level layer: with the role of executing the speed commands generated by other layers of the electronic control system driving the robot motors. Each wheel normally has an independent electronic system, with each motor being controlled by a PID system (Kuc et al., 2001; Oriolo et al., 2002). In the simplest systems, even though the dynamic model is not linear, the driving wheels motors are controlled by PID systems, with gain adjustment to obtain the required responses, response time, etc. under certain working conditions (Cooper, 1995), reliying on the knowledge that the control errors can be corrected by the user in the wheelchair+user control loop.
- high-level layer: the control system provided by the low-level layer is not reliable enough, so other feedback loops are set up to improve its performance, for example, achieving greater precision in the system movements, implementing an adaptive control system for adaptation to changing working conditions or shutting down the system's power consumption. These options have been obtained by implementing classic adaptive control systems (Yu et al., 2003), fuzzy controllers (Espinosa et al., 2001), by means of neural networks (Boquete et al., 2002) or by dynamic feedback linearization (Oriolo et al., 2002), among other possibilities.

The aim of this paper is to improve the basic PID-based speed control of a wheelchair by using another adaptive control loop based on recurrent neural networks. As a result, the overall performance features of the wheelchair (stability, safety, tracking precision, etc.) are improved for being used by other systems of a higher level.

The key advantage of using neural nets in an adaptive control system is that, in most cases, any system can be controlled with a minimum a priori knowledge, and there is no need to obtain the linear plant-defining parameters or the regression matrix. This avoids the need of exhaustive studies beforehand and also makes it possible for the same architecture to be used for solving other control problems with only minor modifications.

Earlier papers presented by the authors described different tests of neural models for the identification and adaptive control of the wheelchair. Boquete et al. (1999a) used a recurrent neural model with FIR/IIR filters as synaptic connections, while in Boquete et al. (1999b) used an internal feedback model between the output and input of each one of the RBF network's neurons, satisfactory results being obtained in both cases. The control algorithms were implemented on a personal computer on the previous mentioned works. In a later paper (Boquete et al., 2002) a specific control-algorithm platform was implemented on a DSP (Digital Signal Processor), while the wheelchair was identified by means of a Kalman filter, which adapts on-line to the wheelchair's characteristics. The experience built up in this earlier work had enabled the development of the algorithms that fed to the solution presented in this paper.

The outline of this paper is as follows: Section 2 describes the neural model used, the training equations and the stability conditions; Section 3 provides a brief survey of the physical characteristics of the system to be controlled; Sections 4 and 5 describe the implementation of two control architectures using the neural model described in Section 2, deriving the equations for the adjustment of the neurocontroller and the stability conditions; Section 6 shows various practical results proving the sound performance of the systems implemented. The paper ends by drawing the main conclusions from this work (Section 7).

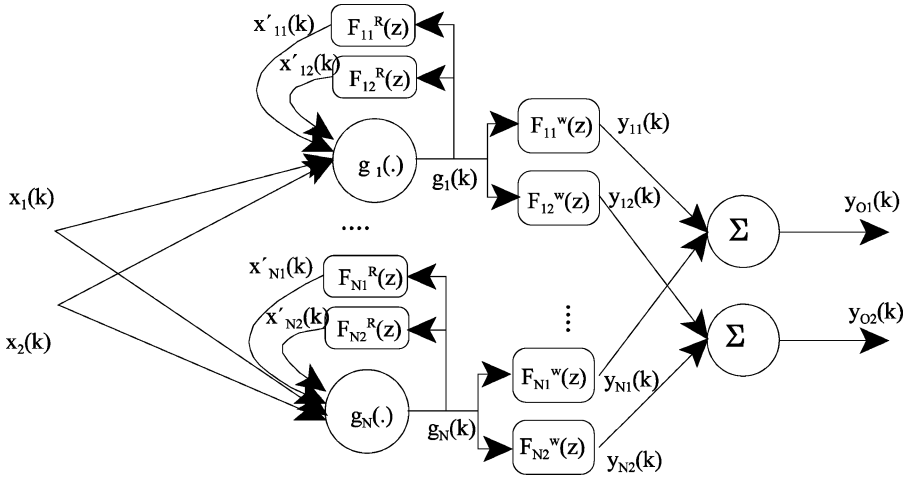

Figure 2. Neural network model.

2. Neural Model

The neural network used is a model with an architecture based on radial basis functions (RBF) using FIR (Finite Impulse Response) filters as feedback and with further FIR filters as synaptic connections (Fig. 2). As can be seen, the proposed model is a hybrid of Chen et al. (1993) (feedback with a filter in each neuron) and Ciocoiu (1996) (using filters as synaptic connections); the main contribution of this paper is the generalisation of the model to systems with any number of inputs and two outputs and the practical application thereof. With a system of two inputs ($x_1(k)$, $x_2(k)$) and two outputs ($y_{O1}(k)$, $y_{O2}(k)$), the model of the radial basis functions is:

$$g_i(k) = e^{-\frac{(x_1(k)+x'_{i1}(k)-C_{i1})^2+(x_2(k)+x'_{i2}(k)-C_{i2})^2}{\sigma^2}} \quad i = 1, \ldots N \quad (2)$$

The centre of each function is $\mathbf{C}_i = (C_{i1}, C_{i2})$ and the functions are evenly distributed over the input space; Φ is a constant modulating the activation zone of each neuron.

Two FIR filters are used for each neuron, connected between its output and each one of its 2 inputs. The output of these filters depends on the previous outputs of each neuron and on the filter coefficients:

$$x'_{im} = \sum_{j=1}^{S} a_{imj} \cdot g_i(k-j) \quad m = 1, 2 \qquad (3)$$

FIR filters are used as synaptic connections so that the past outputs of each neuron are taken into account; the filter between the neuron "i" and the output "p" is:

$$y_{ip}(k) = \sum_{j=0}^{R-1} w_{ipj}(k) \cdot g_i(k-j) \quad p = 1, 2 \qquad (4)$$

Finally, the outputs of the neural model are the sum of the outputs of the filters acting as synaptic connections:

$$y_{Op}(k) = \sum_{i=1}^{N} y_{ip}(k) \qquad (5)$$

As can be seen, the neural model has local activation feedback in each neuron and also local synapse feedback implemented with FIR filters (Tsoi et al., 1994). The error function to be minimised is described by the following equation:

$$\begin{aligned} E(k) &= \frac{1}{2}(y_{O1}(k) - y_{d1}(k))^2 + \frac{1}{2}(y_{O2}(k) - y_{d2}(k))^2 \\ &= \frac{1}{2}e_1^2(k) + \frac{1}{2}e_2^2(k) \end{aligned} \qquad (6)$$

where y_{d1} and y_{d2} are the desired outputs.

The aim of the training phase is to vary the feedback filter coefficients (a_{imj}) and the synaptic filter coefficients (w_{ipj}) to minimise (6). Using the gradient descent technique leads to:

$$\begin{aligned} \Delta w_{ipj}(k) &= -\alpha \cdot \frac{\partial E(k)}{\partial w_{ipj}(k)} \\ &= -\alpha \cdot \frac{\partial E(k)}{\partial y_{Op}(k)} \cdot \frac{\partial y_{Op}(k)}{\partial y_{ip}(k)} \cdot \frac{\partial y_{ip}(k)}{\partial w_{ipj}(k)} \\ &= -\alpha \cdot (y_{Op} - y_{dp}) \cdot g_i(k-j) \end{aligned} \qquad (7)$$

For the feedback filter coefficients:

$$\begin{aligned}\Delta a_{imj}(k) = -\alpha \cdot \frac{\partial E(k)}{\partial a_{imj}(k)} = -\alpha \cdot \left[\frac{\partial E(k)}{\partial y_{O1}(k)}\right. \\ \left. \cdot \frac{\partial y_{O1}(k)}{\partial g_i(k)} + \frac{\partial E(k)}{\partial y_{O2}(k)} \cdot \frac{\partial y_{O2}(k)}{\partial g_i(k)}\right] \\ \cdot \frac{\partial g_i(k)}{\partial a_{imj}(k)} = -\alpha \cdot [(y_{O1}(k) - y_{d1}(k)) \\ \cdot w_{i10} + (y_{O2}(k) - y_{d2}(k)) \cdot w_{i20}] \\ \cdot \left[g_i(k-j) + \sum_{t=1}^{S} a_{imt} \cdot \frac{\partial g_i(k-t)}{\partial a_{imj}}\right] \\ \cdot \frac{\partial g_i(k)}{\partial x'_{im}(k)} \end{aligned} \tag{8}$$

As can be seen in this last equation, adjustment of the neuron's feedback filter coefficients has to be effected by means of a recurrent expression that takes into account the adjustments already made in working cycles before the moment k.

Stability

In this section we find a maximum in the value of the learning factor (α) in such a way as to ensure that the training error $E(k)$ decreases or at least does not increase. A vector $\mathbf{W}$ containing all the adjustable coefficients of the neural network is considered. It can be proved that in a two-output neural network using the gradient descent technique, a sufficient condition for ensuring that $E(k) - E(k-1) \leq 0$ is (see Appendix A):

$$0 < \alpha < \frac{1}{\left\| \frac{\partial y_{Op}(k)}{\partial \mathbf{W}(k)} \right\|^2_{\max}} \tag{9}$$

In the model of Fig. 1 all adjustable coefficients of the neural network have to be considered as elements of $\mathbf{W}$:

$$\mathbf{W} = \left[w_{110}, \ldots w_{N2(R-1)}, a_{111}, \ldots a_{N2S}\right]^T \tag{10}$$

The total number of elements of $\mathbf{W}$ is $2NR + 2NS$, corresponding respectively to the synaptic filters and the feedback filters.

Given that all the elements of $\mathbf{W}$ are limited between $+1$ and -1, we obtain from Eq. (4):

$$\left\| \frac{\partial y_{Op}}{\partial w_{ipj}} \right\|_{\max} = \|g_i(k-j)\|_{\max} = 1 \tag{11}$$

It can be demonstrated that (Boquete et al., 1999a):

$$\left\| \frac{\partial y_{Op}}{\partial a_{imj}} \right\|_{\max} = \frac{M_d}{1 - M_d \cdot S} \tag{12}$$

where

$$M_d = \max \left\| \frac{\partial g_i(k)}{\partial x'_{im}(k)} \right\| = \frac{\sqrt{2}}{\sigma} \cdot e^{-\frac{1}{2}} \tag{13}$$

The following conditions define the region in which the stability of the training process can be assured:

$$\|a_{imj}\| < 1; \quad \|w_{ipj}\| < 1; \quad M_d < \frac{1}{S}; \tag{14}$$

Thus, to ensure convergence in the learning process, the maximum value of the learning factor is:

$$\alpha < \frac{1}{2NR + 2NS\left(\frac{M_d}{1 - S \cdot M_d}\right)^2} \tag{15}$$

In conclusion, this condition ensures that $E(k) - E(k-1) < 0$ over the entire training region, because the Eq. (9) has been obtained in the worst case.

It should be stressed out that this equation is valid only when using the neural network to adjust an error function situated exactly in the network output (for example acting as neuroidentifier of a system). As will be seen in the following sections, if it is used as a neurocontroller, some relevant adjustments need to be made in order to compensate for the variations in the wheelchair dynamics.

3. Characteristics of the Robotic Wheelchair

The wheelchair used in the practical tests is a commercial model which has been equipped with a sensorial system (ultrasound sensors, infrared sensing devices, cameras, etc.) which facilitate its guidance. There are also different user-operated control modes (joystick, vocal commands, air expulsion, eye movements) and various user interfaces. The mechanical structure of the wheelchair consists of a platform (measuring 100 × 80 × 58 cm, and weighing approximately 35 Kg) on two driving wheels and two castor wheels. The motor wheels, with a radius $R_d = 16$ cm and separated by a distance $D = 54$ cm, have independent traction provided by two DC motors.

To control the rotation speeds of the right-hand and left-hand wheels, an electronic system was implemented for each wheel, based on PID control of

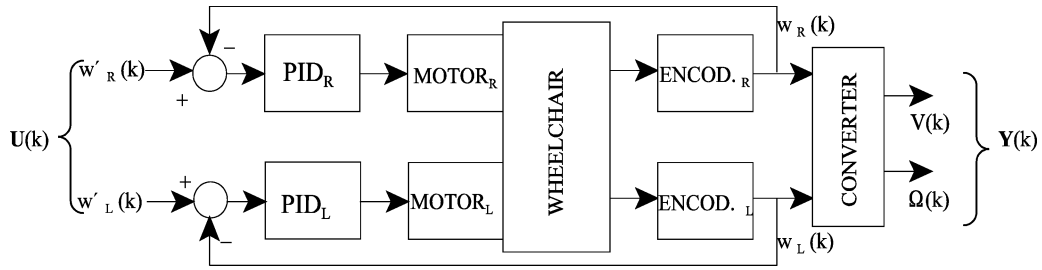

Figure 3. Low level control.

the motors of said wheels (Fig. 3). This low-level control layer made possible, by means of the suitable commands, to ensure that the angular speed of the righthand and lefthand wheels (w_R, w_L) was approximately the same as that indicated on the electronic control card:

$$\begin{aligned} w'_R &\simeq w_R \\ w'_L &\simeq w_L \end{aligned} \tag{16}$$

In the model of our plant a system is also included (converter) to convert the angular speeds of the wheels, obtained from the reading and integration of the data from each of the encoders, into the linear speed ($V(k)$) and the angular speed ($\Omega(k)$).

For our purposes, therefore, the plant input is the vector $\mathbf{U}(k) = [w'_R(k), w'_L(k)]^T$ and the output is $\mathbf{Y}(k) = [V(k), \Omega(k)]^T$.

4. Inverse Control by Calculating the Jacobian

Two neural control schemes for governing the wheelchair movements were implemented, both using the neural model of Fig. 1. The first scheme (Scheme I) takes into account the effect of the PID control of the wheelchair motors and carries out a simple analysis of its dynamics to obtain, approximately, the relation between linear and angular speed of the mobile robot and the command provided to the input of the PID controller.

$$\begin{aligned} V(k) &= \frac{R_d}{2} \cdot [w_R(k) + w_L(k)] \\ &\quad + G_1[V(k-1), V(k-2), \ldots \Omega(k-1) \ldots] \\ \Omega(k) &= \frac{R_d}{D} \cdot [w_R(k) - w_L(k)] \\ &\quad + G_2[V(k-1), V(k-2), \ldots \Omega(k-1) \ldots] \end{aligned} \tag{17}$$

$G_1(\cdot)$ and $G_2(\cdot)$ represent the nonlinear response of the wheelchair. These equations then serve as the basis for obtaining the expression of the sensitivity of each output to each of the system inputs:

$$\begin{aligned} \begin{bmatrix} J_{11} & J_{12} \\ J_{21} & J_{22} \end{bmatrix} &= \begin{bmatrix} \frac{\partial V}{\partial w'_R}(k) & \frac{\partial V}{\partial w'_L}(k) \\ \frac{\partial \Omega}{\partial w'_R}(k) & \frac{\partial \Omega}{\partial w'_L}(k) \end{bmatrix} = \begin{bmatrix} \frac{R_d}{2} & \frac{R_d}{2} \\ \frac{R_d}{D} & -\frac{R_d}{D} \end{bmatrix} \\ &= \begin{bmatrix} \frac{0,16}{2} & \frac{0,16}{2} \\ \frac{0,16}{0,54} & -\frac{0,16}{0,54} \end{bmatrix} \end{aligned} \tag{18}$$

The interesting aspect of this expression is the sign of each one of the terms, not the absolute value; accordingly, that it would even be possible to work with values of $+1$ and -1.

Figure 4 shows the classic model-oriented control structure, which uses a neurocontroller (this generates the control signal ($\mathbf{U}$(k)) on the basis of the reference signals ($V_d(k), \Omega_d(k)$)), a reference model (with output $V_m(k), \Omega_m(k)$), and an adjustment algorithm for minimizing the control error $E(k)$. The variables involved are:

$$\begin{aligned} \mathbf{Y}(k) &= \begin{bmatrix} V(k) \\ \Omega(k) \end{bmatrix} \quad \mathbf{R}(k) = \begin{bmatrix} V_d(k) \\ \Omega_d(k) \end{bmatrix} \\ \mathbf{U}(k) &= \begin{bmatrix} w'_R(k) \\ w'_L(k) \end{bmatrix} \quad \mathbf{Y}_m(k) = \begin{bmatrix} V_m(k) \\ \Omega_m(k) \end{bmatrix} \end{aligned} \tag{19}$$

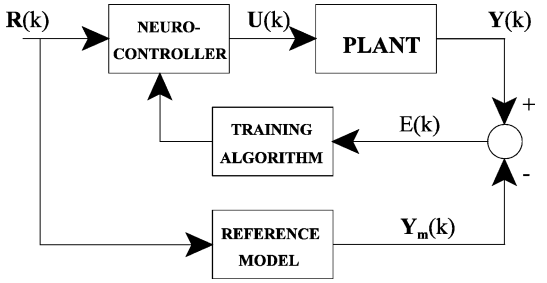

Figure 4. Control Scheme I.

Note how the excitation of the wheelchair is produced on variables w'_R and w'_L, which are the inputs to the PID control system. The error function to be minimized is the difference between the real output of the plant ($\mathbf{Y}(k)$) and the output given by the reference model:

$$E(k) = \frac{1}{2}(V(k) - V_m(k))^2 + \frac{1}{2}(\Omega(k) - \Omega_m(k))^2 \tag{20}$$

The neurocontroller + wheelchair unit may be considered to be a single multi-layer neural network, in which the coefficients of the physical system are obviously not modified at the moment of applying the error backpropagation algorithm. However, this last layer must serve to obtain the sensitivity of the response of the plant and appropriately adjust the coefficients of the neurocontroller. In this way, the formulas for the adjustment of the neurocontroller are:

$$\begin{aligned}\Delta w_{ipj}(k) &= -\alpha \cdot \frac{\partial E(k)}{\partial w_{ipj}(k)} \\ &= -\alpha \cdot [e_1(k) \cdot J_{11} + e_2(k) \cdot J_{21}] \cdot \frac{\partial w'_R(k)}{\partial w_{ipj}(k)} \\ &\quad -\alpha \cdot [e_1(k) \cdot J_{12} + e_2(k) \cdot J_{22}] \cdot \frac{\partial w'_L(k)}{\partial w_{ipj}(k)} \\ &= -\alpha [e_1(k) \cdot J_{1P} + e_2(k) \cdot J_{2P}] \cdot \frac{\partial y_{OP}}{\partial w_{ipj}}\end{aligned} \tag{21}$$

$$\begin{aligned}\Delta a_{imj}(k) &= -\alpha \cdot \frac{\partial E(k)}{\partial a_{imj}(k)} \\ &= -\alpha \cdot [e_1(k) \cdot J_{11} + e_2(k) \ \cdot J_{21}] \cdot \frac{\partial w'_R(k)}{\partial a_{imj}(k)} \\ &\quad -\alpha \cdot [e_1(k) \cdot J_{12} + e_2(k) \cdot J_{22}] \cdot \frac{\partial w'_L(k)}{\partial a_{imj}(k)} \\ &= -\alpha [e_1(k) \cdot J_{1P} + e_2(k) \cdot J_{2P}] \cdot \frac{\partial y_{OP}}{\partial a_{imj}}\end{aligned} \tag{22}$$

where

$$\begin{aligned} e_1(k) &= (V(k) - V_m(k)) \quad e_2(k) = (\Omega(k) - \Omega_m(k)) \\ w'_R(k) &= y_{O1}(k) \quad w'_L(k) = y_{O2}(k)\end{aligned} \tag{23}$$

Stability

Applying the result indicated by Eq. (9) and considering the neurocontroller+wheelchair unit to be a single neural network, the following conditions must be fulfilled by the control system of Fig. 4:

$$0 < \alpha < \frac{1}{\left\| \frac{\partial V(k)}{\partial \mathbf{W}} \right\|^2_{\max}} \quad 0 < \alpha < \frac{1}{\left\| \frac{\partial \Omega(k)}{\partial \mathbf{W}} \right\|^2_{\max}} \tag{24}$$

Equation (18) has to be taken into account to obtain the expressions of Eq. (24):

$$\begin{aligned}\left\| \frac{\partial V(k)}{\partial w_{ipj}} \right\|_{\text{máx}} &= \left\| \frac{\partial V(k)}{\partial w'_R} \frac{\partial w'_R}{\partial w_{ipj}} + \frac{\partial V(k)}{\partial w'_L} \frac{\partial w'_L}{\partial w_{ipj}} \right\|_{\text{máx}} \\ &= \left\| \frac{\partial V(k)}{\partial y_{Op}} \frac{\partial y_{Op}}{\partial w_{ipj}} \right\| = \|J_{1p}\|_{\text{máx}} = \frac{R_d}{2}\end{aligned} \tag{25}$$

$$\begin{aligned}\left\| \frac{\partial \Omega(k)}{\partial w_{ipj}} \right\|_{\text{máx}} &= \left\| \frac{\partial \Omega(k)}{\partial w'_R} \frac{\partial w'_R}{\partial w_{ipj}} + \frac{\partial \Omega(k)}{\partial w'_L} \frac{\partial w'_L}{\partial w_{ipj}} \right\|_{\text{máx}} \\ &= \left\| \frac{\partial \Omega(k)}{\partial y_{Op}} \frac{\partial y_{Op}}{\partial w_{ipj}} \right\|_{\max} = \|J_{2p}\|_{\text{máx}} = \frac{R_d}{D}\end{aligned} \tag{26}$$

As the most unfavourable condition, Eq. (26) must be chosen. Calculating the maximum sensitivity of the outputs of the wheelchair with respect to the coefficients of the feedback filters, and taking into consideration Eq. (12):

$$\begin{aligned}\left\| \frac{\partial V(k)}{\partial a_{imj}} \right\|_{\text{máx}} &= \left\| J_{11} \cdot \frac{\partial w'_R}{\partial a_{imj}} + J_{12} \cdot \frac{\partial w'_L}{\partial a_{imj}} \right\|_{\text{máx}} \\ &= R_d \cdot \frac{M_d}{1 - M_d \cdot S}\end{aligned} \tag{27}$$

$$\begin{aligned}\left\| \frac{\partial \Omega(k)}{\partial a_{imj}} \right\|_{\text{máx}} &= \left\| \frac{R_d}{D} \frac{\partial w'_R}{\partial a_{imj}} - \frac{R_d}{D} \frac{\partial w'_L}{\partial a_{imj}} \right\|_{\text{máx}} \\ &= [\|J_{21}\|_{\max} + \|J_{22}\|_{\max}] \frac{M_d}{1 - M_d S} \\ &= \frac{2R_d}{D} \cdot \frac{M_d}{1 - M_d \cdot S}\end{aligned} \tag{28}$$

With the physical values of the wheelchair, the most unfavourable case is that indicated by Eq. (28). In short, the maximum value of the learning factor that can be used in the control system of Fig. 4 is:

$$0 < \alpha < \frac{1}{2 \cdot N \cdot R \cdot \left(\frac{R_d}{D}\right)^2 + 2N \cdot S \cdot \left(2\frac{R_d}{D} \cdot \frac{M_d}{1 - M_d \cdot S}\right)^2} \tag{29}$$

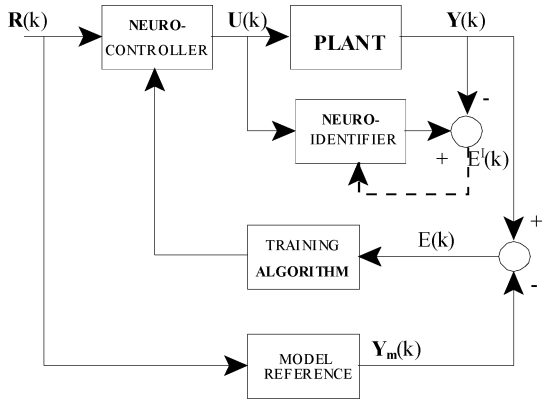

Figure 5. Control scheme using a neuroidentifier.

5. Inverse Control Using a Neuroidentifier

Figure 5 shows the second option of inverse control (Scheme II), using in this case another neural network (similar to that of Fig. 1) in parallel with the wheelchair, so that the latter serves as a path for propagating the control error to the neurocontroller. The neuroidentifier serves for obtaining in each sampling time (k) the plant's model. This model will be useful for propagating the control error from the output to the neurocontroller. The advantage of this scheme is that no assumption has to be made about the dynamics of the wheelchair, so the same scheme can be valid for controlling any 2-input, 2-output system.

In each working cycle (k) two functions have to be minimised: the identification error $E^I(k)$ and the control error $E(k)$ (Eq. (20)). The first is defined as:

$$E^I(k) = \frac{1}{2}\left(y^I_{O1}(k) - V(k)\right)^2 + \frac{1}{2}\left(y^I_{O2}(k) - \Omega(k)\right)^2 \tag{30}$$

The superscript "I" indicates neuroidentifier coefficients. The neuroidentifier is adjusted in each working cycle by means of Eqs. (7) and (8), considering the linear speed and angular speed of the wheelchair, respectively, to be the desired network outputs.

When the identifier error is negligible, the transfer function of the neuroidentifier coincides with the wheelchair model, and the following information can therefore be obtained:

$$J_{pm}(k) = -2 \cdot \sum_{i=1}^{N^I} \frac{x^I_m + x'^I_{im}(k) - C^I_{im}}{\sigma^{I^2}} \cdot w^I_{ip0} \cdot g^I_i(k) \tag{31}$$

As a consequence, Eqs. (21) and (22) can be used for the adjustment of the neurocontroller.

We also need to calculate the absolute maximum value of J_{pm}, which comes out as:

$$\|J_{pm}(k)\|_{\max} = 2 \cdot N^I \cdot M^I_d \tag{32}$$

Stability

To obtain the maximum value of the learning factor used in the control scheme shown in Fig. 5, expression 9 is applied, given that in each learning cycle the neurocontroller and neuroidentifier coefficients are adjusted; for stability purposes, both networks are considered to form a multilayer network, leading to the following vector $\mathbf{W}$:

$$\mathbf{W} = \left[w_{110}, \ldots w_{N2(R-1)}, a_{111}, \ldots a_{N2S}, w^I_{110}, \ldots w^I_{N^I 2(R^I-1)}, a^I_{111}, \ldots a^I_{N^I 2S^I}\right]^T \tag{33}$$

The number of elements of the vector $\mathbf{W}$ is $2NR + 2NS + 2N^I R^I + 2N^I S^I$, corresponding to the neurocontroller and neuroidentifier respectively. From Eqs. (11) and (12):

$$\left\|\frac{\partial y^I_{Op}}{\partial w^I_{ipj}}\right\|_{\max} = \left\|g^I_i(k-j)\right\|_{\max} = 1 \tag{34}$$

$$\left\|\frac{\partial y^I_{Op}}{\partial a^I_{imj}}\right\|_{\max} = M^I_d \cdot \frac{1}{1 - M^I_d \cdot S^I} \tag{35}$$

The expressions (26) and (28) are valid for coefficients of the neurocontroller, considering the value of the Jacobians to be given by the expression (31).

$$\left\|\frac{\partial y^I_{Op}}{\partial w_{ipj}}\right\|_{\max} = 2 \cdot M^I_d \cdot N^I \tag{36}$$

$$\left\|\frac{\partial y^I_{Op}}{\partial a_{imj}}\right\|_{\max} = \frac{M_d}{1 - M_d \cdot S} \cdot 4 \cdot M^I_d \cdot N^I \tag{37}$$

The following conditions have to be met:

$$M_d < \frac{1}{S}; \quad M^I_d < \frac{1}{S^I}; \quad \|w_{ipj}\| < 1; \quad \left\|w^I_{ipj}\right\| < 1; \quad \|a_{imj}\| < 1; \quad \left\|a^I_{imj}\right\| < 1; \tag{38}$$

In short, the maximum value of the learning factor to be used in the control scheme of Fig. 5 is:

$$0 < \alpha < \frac{1}{2N^I R^I + 2N^I \cdot S^I \cdot \left(\frac{M_d^I}{1-M_d^I \cdot S^I}\right)^2 + 2NR\left(2M_d^I \cdot N^I\right)^2 + 2N \cdot S \cdot \left(\frac{M_d}{1-M_d \cdot S} \cdot 4M_d^I \cdot N^I\right)^2} \tag{39}$$

6. Practical Tests

This section gives some practical results of the control of the robotic wheelchair for disabled people. Both architectures were implemented in a specific hardware system based on a DSP, small enough in terms of size and energy consumption to be fitted on a wheelchair (Boquete et al., 2002). The number of sampling cycles is not limited by this hardware system but rather by the communication bus used for communicating the various wheelchair elements. The rate of 12 samples per second is sufficient time for controlling a system with the inertia of a wheelchair. Several tests were conducted for each of the two control architectures to find out the configuration (number of neurons, number of filter coefficients, etc.) that gave the best results, always respecting the stability conditions.

Two examples of wheelchair behaviour are shown for each one of the architectures: movement in a straight line at constant speed ($V = 37.7$ cm/s, $\Omega = 0$ rd/s); in the second example the wheelchair describes a circular trajectory with a radius of 1 m; this trajectory is obtained with the following commands: $V = 37.7$ cm/s, $\Omega = 0.38$ rd/s, which are based on the physical dimensions of the wheelchair. In all the tests there was a person weighing 62 kg seated therein. The equation of the reference model is the same as that used in Narendra and Parthasarathy (1990):

$$\begin{aligned} V_m(k) &= \beta \cdot V_m(k-1) + V_d(k) \\ \Omega_m(k) &= \beta \cdot \Omega_m(k-1) + \Omega_d(k) \\ |\beta| &= 0.7 < 1 \end{aligned} \tag{40}$$

The centres of the exponential functions were equally distributed in the square defined by the points $(-1, -1)$ and (1, 1), thereby also standardising the input signals to the neural network.

First Control Scheme. When using the inverse control by calculating the jacobian, the configuration used is defined by the following parameters:

$$N = 9 \quad \sigma = 2.0 \quad R = 2 \quad S = 2 \quad \alpha = 0.05$$

Figures 6 and 7 show the results obtained when the robotic wheelchair describes a straight-line trajectory and a circular trajectory, respectively. At the start ($k = 0$) the neurocontroller coefficients are randomly selected; as can be seen, the control error is minimal after very few working cycles and the movements of the robotic wheelchair are governed with high reliability. It should be pointed out that the error during the first instants of time is largely due to the fact that the wheelchair's caster wheels are not properly aligned for the movement the wheelchair is to generate, and it takes 2 to 4 seconds to line up correctly.

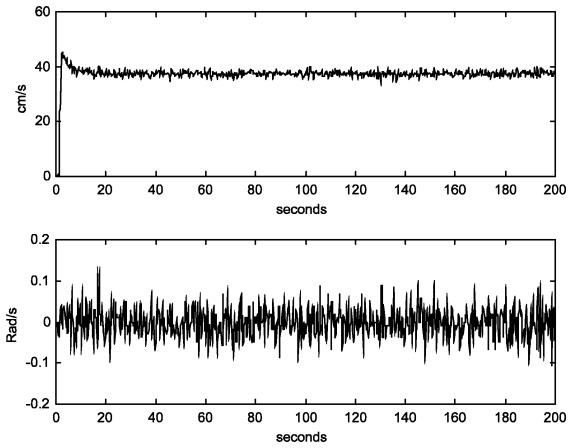

Figure 6. Avancing in a straight forward movement (Scheme I).

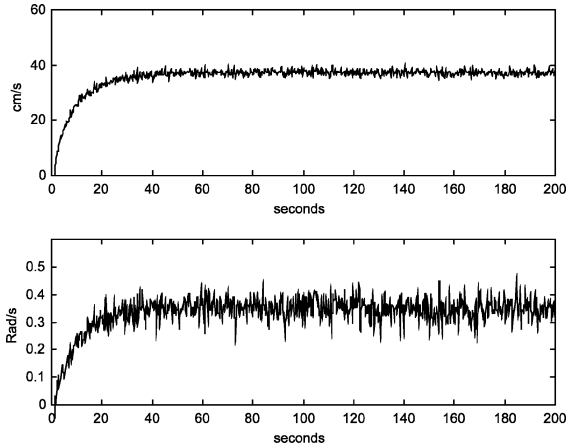

Figure 7. Describing a circunference (Scheme I).

Table 1. Wheelchair describing a circular movement (Scheme I).

Variable	Mean value	Standard deviation
V	$V = 36.29$ cm/s	$V = 2.13$ cm/s
Ω	$\Omega = 0.37$ rd/s	$\Omega = 0.034$ rd/s

To facilitate the comparison of results, Table 1 shows the behaviour of the 2 wheelchair variables after taking the average of 5 experiments while the wheelchair is describing a circular movement. The mean value and standard deviation have been measured from the instant $t = 0$ to $t = 200$ sg.

Second Control Scheme. For this test, the following set of parameters are used:

$$N = 9 \quad \sigma = 2.0 \quad R = 2 \quad S = 2 \quad \alpha = 0.000004$$
$$N^I = 9 \quad \sigma^I = 2.0 \quad R^I = 2 \quad S^I = 2$$

The practical results are shown in Figs. 8 and 9; it should be pointed out that the neuroidentifier was preadjusted before being implemented in the control architecture, so that it would approximate the wheelchair dynamics. The results for the circular movement are as follows (Table 2), obtained under the same conditions as in the previous subsection.

As can be seen, the behaviour is worse that achieved in the first control scheme, doubtless due to the need for the identification error between the plant and the neuroidentifier to be reduced to values that allow an optimum adjustment of the neurocontroller parameters.

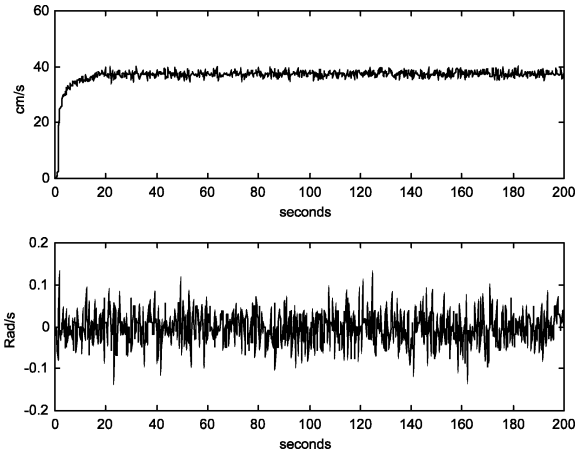

Figure 8. Avancing in a straight forward movement (Scheme II).

Table 2. Describing a circular movement (Scheme II).

Variable	Mean value	Standard deviation
V	$V = 35.4$ cm/s	$V = 2.9$ cm/s
Ω	$\Omega = 0.39$ rd/s	$\Omega = 0.049$ rd/s

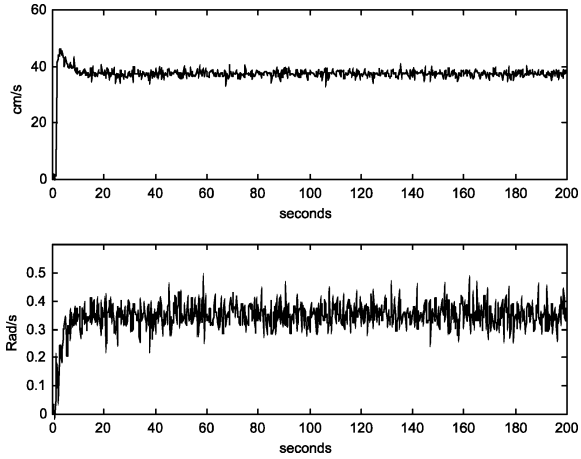

Figure 9. Describing a circunference (Scheme II).

Effect of the Parameters on the Response. In all the practical examples, a smooth response without overshooting was achieved from initial to final values, although quicker or slower responses can be obtained by varying the parameters of the control scheme. An analysis of any of the equations that establish the stability of the control system shows that the response speed can be regulated by varying the value of the learning factor ($\forall$) or the number of neurons or coefficients defining various neural models. Nonetheless, it should be borne in mind that it implies the risk of making the control system unstable.

For example, using the Scheme I, Figs. 10 and 11 show the effect on the response of different values of α; the higher the learning factor, the more the system oscillates, since with high increments, the function to be minimised tends to oscillate around the minimum; on the other hand, if a small value of i is used, the error takes a long time to settle down at an acceptable value.

Figures 12 and 13 show the wheelchair response when the number of neurocontroller neurons is varied. The greater the number of neurons, the quicker the system response.

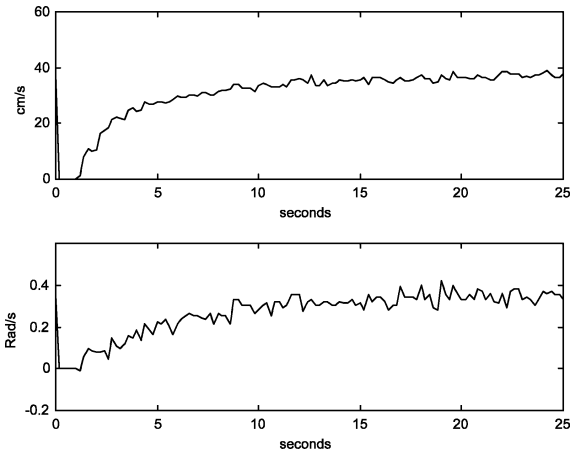

Figure 10. Response with $\alpha = 0.02$.

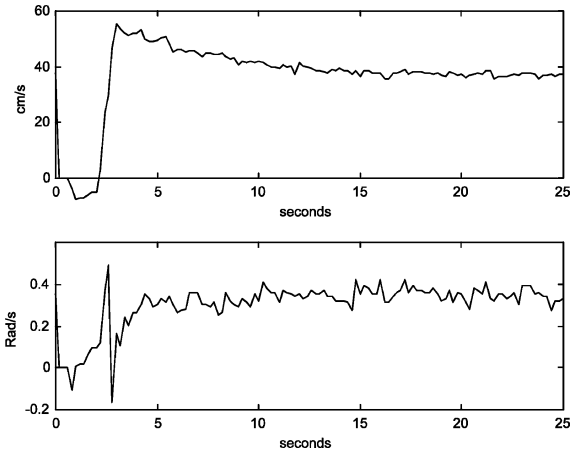

Figure 11. Response with $\alpha = 0.05$.

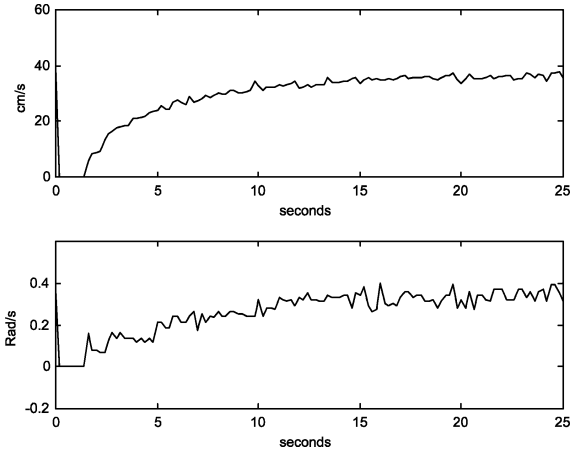

Figure 12. Response with $N = 9$.

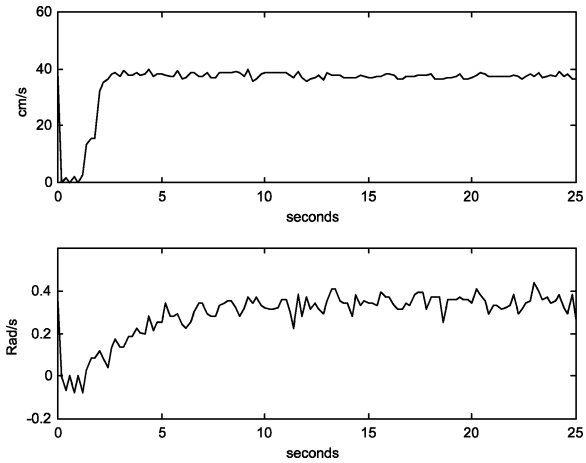

Figure 13. Response with $N = 25$.

Similar curves can be obtained by varying the number of filter coefficients or modifying the value of σ. By choosing the suitable parameter, users can thus adjust the wheelchair response to their special characteristics.

Example of Adaptive Control. Another set of practical tests aimed to check the behaviour of the robotic wheelchair movement control system when there was a sudden change in its working conditions and hence observe how the system adapts to new working conditions. The test consists in giving the wheelchair the commands to describe a circular trajectory. At first, the wheelchair is empty and at a given moment (after 80 seconds) a person weighing 62 kg sits down in it without stopping its movement; and after 115 seconds gets up. Figure 14 shows an example of one of these experiments using control Scheme I. As can be seen, after the transient at the moment when the working conditions vary, the control system settles down in very few working cycles and governs the wheelchair correctly again. In Tables 3 and 4 the main results of this experiment using Schemes I and II are given.

Comparison with Other Control Possibilities. In this section the system is compared with the behaviour of control systems set up with other options to show its

Table 3. Adaptive neural control (Scheme I).

Variable	Mean value	Standard deviation
V	$V = 35.83$ cm/s	$V = 3.57$ cm/s
Ω	$\Omega = 0.39$ rd/s	$\Omega = 0.059$ rd/s

Table 4. Adaptive neural control (Scheme II).

Variable	Mean value	Standard deviation
V	$V = 35.12$ cm/s	$V = 3.90$ cm/s
Ω	$\Omega = 0.40$ rd/s	$\Omega = 0.071$ rd/s

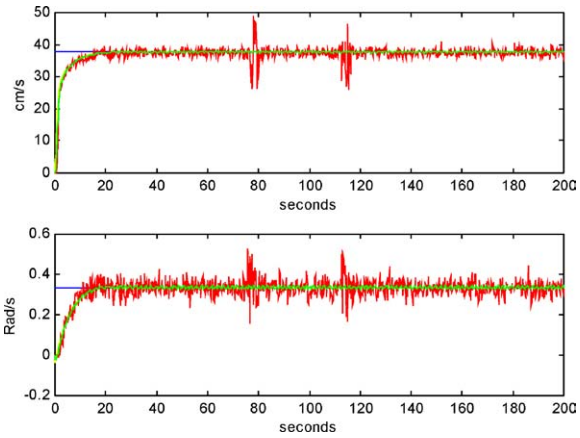

Figure 14. Example of adaptive control.

advantages. For these tests the movement commands given to the wheelchair are intended again to follow a circular trajectory with a person weighing 62 kg seated therein. The results shown correspond to the average value taken after carrying out each test 5 times.

Comparison with PID Control. Forced equality in any of the control schemes $\mathbf{U}(k) = \mathbf{R}(k)$ annuls the neurocontroller effect; in other words the wheelchair is then governed by the low level PID system. Under these conditions and forcing the generation of a circular trajectory the following results are obtained (Table 5).

These results are clearly inferior to those obtained in any of the neural control configurations described herein. This behaviour difference is exacerbated when the wheelchair is subject to sudden changes in its dynamic model; the test defined above for observing the control system's behaviour when there is a sudden change in the system mass, but this time with PID-based control gives the results shown in Table 6.

Table 5. PID control.

Variable	Mean value	Standard deviation
V	$V = 33.6$ cm/s	$V = 4.1$ cm/s
Ω	$\Omega = 0.37$ rd/s	$\Omega = 0.091$ rd/s

Table 6. Adaptive control with PID.

Variable	Mean value	Standard deviation
V	$V = 33.9$ cm/s	$V = 5.2$ cm/s
Ω	$\Omega = 0.39$ rd/s	$\Omega = 0.122$ rd/s

This shows how the quality of the control system decreased when using only PID control; the conclusion to be drawn from this is that the neural control system adapts better than the PID control system to plant parameter changes.

Tests with Other Neural Models. Previous papers published by the authors dealt with different neural models from those presented herein and also different identifiers (Kalman filter). A summary of the results is given below. It can clearly be seen that these results have been improved by the system proposed herein. For the sake of simplification the results are shown only of the adaptive control experiment described so far.

By acting on the parameters defining the structure of the neural network, it is possible to simulate other neural network models, either recurrent or non-recurrent. For example, the configuration ($R = 1, a_{imj} = 0$) gives non-recurrent networks; the configuration ($a_{imj} = 0$) eliminates the feedback recurrence in each of the neurons; the option $R = 1$ possibility gives synaptic connections without memory. All these possibilities have been tested for the control of wheelchairs in previous papers published by the authors, obtaining results that are inferior to those presented herein. A summary of the results is given below:

In the first paper (Boquete et al., 1999a) the wheelchair was controlled by the control Scheme I; the neural architecture was based on an RBF with synaptic connections without memory ($R = 1$) but with FIR filters as feedback for each neuron ($S = 2$). The Table 7 sums up the results (adaptive control).

In another of the possibilities analysed (Boquete et al., 1999b) FIR filters with synaptic connections were used but without feedback for each neuron ($a_{imj} = 0$),

Table 7. Adaptive control test with synaptic connections without memory ($R = 1$, $S = 2$).

Variable	Mean value	Standard deviation
V	$V = 36.35$ cm/s	$V = 3.92$ cm/s
Ω	$\Omega = 0.38$ rd/s	$\Omega = 0.068$ rd/s

Table 8. Adaptive control test with $a_{imj} = 0$ (control Scheme II).

Variable	Mean value	Standard deviation
V	$V = 35.27$ cm/s	$V = 4.22$ cm/s
Ω	$\Omega = 0.37$ rd/s	$\Omega = 0.072$ rd/s

Table 9. Adaptive control using a Kalman filter as identifier.

Variable	Mean value	Standard deviation
V	$V = 36.11$ cm/s	$V = 4.27$ cm/s
Ω	$\Omega = 0.037$ rd/s	$\Omega = 0.092$ rd/s

implementing the control Scheme II. Again we show the test results (Table 8).

Lastly, in Boquete et al. (2002) Scheme II was used but without a neuroidentifier. A linear system was used as plant's identifier (Kalman filter), also updated in each operation cycle of the complete system. The Table 9 shows the results, which are slightly worse than those obtained in this paper.

The use of a Kalman filter as wheelchair identifier makes possible to consider the wheelchair identification process as a linear one. This is not necessary in the solutions proposed herein.

7. Conclusions

This paper shows a practical case of control of a real system (wheelchair for disabled people) by means of a neural system using a new architecture of recurrent neural network based on a RBF model. Equations for adjusting the coefficients (FIR filters) were obtained as well as the stability conditions for 2-output models. Two different wheelchair control architectures were then implemented, obtaining totally satisfactory results in both cases, using learning parameters that ensure system stability. The first architecture calls for fewer calculations, at the cost of having to carry out a study of the dynamics of the system to be controlled; the main characteristic of the control architecture using a neuroidentifier (Scheme II) is that it can be used for controlling any physical system with 2 inputs and 2 outputs. Nonetheless, coefficients of the neuroidentifier and neurocontroller need to be adjusted at each sampling step.

A study was made of the behaviour of one of the control systems when its architecture parameters were varied, showing that it is possible to vary the response speed of the control system by varying the training parameters or the architecture of the neurocontroller. Lastly, a comparison between the different control systems implemented and other control systems is made; the conclusion is that better results are obtained with the new possibility presented herein.

We consider the main conclusions of this article to be the following:

1. Design of a new model of recurrent neural network with the adjustment equations being obtained by the gradient descent algorithm; the stability conditions obtained in the training region ensure that all **W** elements have a maximum modulus value of unity.
2. Use of the model obtained in 2 control systems; in this case the control system's stability conditions have also been established in closed loop. The system's stability conditions have been obtained using the robotic wheelchair's characteristics.
3. Demonstration of its correct performance in implementing the adaptive control of the movements of a wheelchair, a system characterised by brusque changes in working conditions. The set of tests carried out show the system's behaviour response to changes in training conditions that might affect the stability of the complete system. This improves the results obtained using other control techniques.
4. Implementation of the control system on low-complexity hardware. The wheelchair is controlled by a classic PID system and the neural control algorithms can be implemented on a DSP or a microprocessor with average performance features.

Appendix A: Proof of Eq. (9)

In this section we find a maximum in the value of the learning factor ($\forall$) in such a way that it ensures that the training error decreases at all times: $E(k+1) - E(k) < 0$. For this purpose a vector **W** containing all the adjustable coefficients of the neural network is considered.

The variation in vector **W** is:

$$\begin{aligned}\Delta\mathbf{W}(k) &= -\alpha[y_{O1}(k) - y_{d1}(k)]\frac{\partial y_{O1}(k)}{\partial \mathbf{W}(k)} \\ &\quad -\alpha[y_{O2}(k) - y_{d2}(k)]\frac{\partial y_{O2}(k)}{\partial \mathbf{W}(k)} \\ &= -\alpha e_1(k)\frac{\partial y_{O1}(k)}{\partial \mathbf{W}(k)} - \alpha e_2(k)\frac{\partial y_{O2}(k)}{\partial \mathbf{W}(k)} \qquad (41)\end{aligned}$$

The increment in function $E(k)$ es:

$$\begin{aligned}\Delta E(k) &= E(k+1) - E(k)\\ &= \frac{1}{2}\left[e_1^2(k+1) + e_2^2(k+1) - e_1^2(k) - e_2^2(k)\right]\\ &= \Delta e_1(k)\left[e_1(k) + \frac{1}{2}\Delta e_1(k)\right]\\ &\quad + \Delta e_2(k)\left[e_2(k) + \frac{1}{2}\Delta e_2(k)\right]\end{aligned} \tag{42}$$

The respective increments in $e_1(k)$ and $e_2(k)$ are due to the difference in vector $\mathbf{W}$:

$$\begin{aligned}\Delta e_1(k) &\simeq \left[\frac{\partial e_1(k)}{\partial \mathbf{W}(k)}\right]^T \cdot \Delta \mathbf{W}(k)\\ \Delta e_2(k) &\simeq \left[\frac{\partial e_2(k)}{\partial \mathbf{W}(k)}\right]^T \cdot \Delta \mathbf{W}(k)\end{aligned} \tag{43}$$

From Eq. (6)

$$\frac{\partial e_p(k)}{\partial \mathbf{W}(k)} = \frac{\partial y_{Op}(k)}{\partial \mathbf{W}(k)} \quad p = 1, 2 \tag{44}$$

we obtain

$$\begin{aligned}\Delta e_1(k) = &-\alpha e_1(k)\left[\frac{\partial y_{O1}(k)}{\partial \mathbf{W}(k)}\right]^T \cdot \frac{\partial y_{O1}(k)}{\partial \mathbf{W}(k)}\\ &-\alpha e_2(k)\left[\frac{\partial y_{O1}(k)}{\partial \mathbf{W}(k)}\right]^T \cdot \frac{\partial y_{O2}(k)}{\partial \mathbf{W}(k)}\end{aligned} \tag{45}$$

and

$$\begin{aligned}\Delta e_2(k) = &-\alpha e_2(k)\left[\frac{\partial y_{O2}(k)}{\partial \mathbf{W}(k)}\right]^T \cdot \frac{\partial y_{O2}(k)}{\partial \mathbf{W}(k)}\\ &-\alpha e_1(k)\left[\frac{\partial y_{O2}(k)}{\partial \mathbf{W}(k)}\right]^T \cdot \frac{\partial y_{O1}(k)}{\partial \mathbf{W}(k)}\end{aligned} \tag{46}$$

The increment in function $E(k)$ is

$$\begin{aligned}\Delta E(k) = &-\alpha e_1^2(k)\left\|\frac{\partial y_{O1}}{\partial \mathbf{W}(k)}\right\|^2 - \alpha e_2^2(k)\left\|\frac{\partial y_{O2}}{\partial \mathbf{W}(k)}\right\|^2\\ &-2\alpha e_1(k)e_2(k)\left[\frac{\partial y_{O1}}{\partial \mathbf{W}(k)}\right]^T \frac{\partial y_{O2}}{\partial \mathbf{W}(k)}\\ &+\frac{1}{2}\left[\alpha e_1(k)\left\|\frac{\partial y_{O1}}{\partial \mathbf{W}(k)}\right\|^2\right.\\ &\left.+\alpha e_2(k)\left[\frac{\partial y_{O1}}{\partial \mathbf{W}(k)}\right]^T \frac{\partial y_{O2}}{\partial \mathbf{W}(k)}\right]^2\\ &+\frac{1}{2}\left[\alpha e_2(k)\left\|\frac{\partial y_{O2}}{\partial \mathbf{W}(k)}\right\|^2\right.\\ &\left.+\alpha e_1(k)\left[\frac{\partial y_{O1}}{\partial \mathbf{W}(k)}\right]^T \frac{\partial y_{O2}}{\partial \mathbf{W}(k)}\right]^2\end{aligned} \tag{47}$$

The above equation can be written as follows:

$$\begin{aligned}\Delta E(k) = &-\alpha\left[e_1(k)\frac{\partial y_{O1}}{\partial \mathbf{W}(k)} + e_2(k)\frac{\partial y_{O2}}{\partial \mathbf{W}(k)}\right]^2\\ &+\frac{1}{2}\left[\alpha e_1(k)\left\|\frac{\partial y_{O1}}{\partial \mathbf{W}}\right\|^2 + \alpha e_2(k)\left[\frac{\partial y_{O1}}{\partial \mathbf{W}}\right]^T \frac{\partial y_{O2}}{\partial \mathbf{W}}\right]^2\\ &+\frac{1}{2}\left[\alpha e_2(k)\left\|\frac{\partial y_{O2}}{\partial \mathbf{W}}\right\|^2 + \alpha e_1(k)\left[\frac{\partial y_{O1}}{\partial \mathbf{W}}\right]^T \frac{\partial y_{O2}}{\partial \mathbf{W}}\right]^2\end{aligned} \tag{48}$$

The last expression can be made negative in the following way:

$$\begin{aligned}&\alpha\left[e_1(k)\frac{\partial y_{O1}}{\partial \mathbf{W}(k)} + e_2(k)\frac{\partial y_{O2}}{\partial \mathbf{W}(k)}\right]^2\\ &> \frac{1}{2}\alpha^2\left[\left[\frac{\partial y_{O1}}{\partial \mathbf{W}}\right]^T \cdot \left(e_1(k)\frac{\partial y_{O1}}{\partial \mathbf{W}} + e_2(k)\frac{\partial y_{O2}}{\partial \mathbf{W}}\right)\right]^2\\ &\quad + \frac{1}{2}\alpha^2\left[\left[\frac{\partial y_{O2}}{\partial \mathbf{W}}\right]^T \cdot \left(e_1(k)\frac{\partial y_{O1}}{\partial \mathbf{W}} + e_2(k)\frac{\partial y_{O2}}{\partial \mathbf{W}}\right)\right]^2\\ &\quad + \alpha\left\|e_1(k)\frac{\partial y_{O1}}{\partial \mathbf{W}} + e_2(k)\frac{\partial y_{O2}}{\partial \mathbf{W}}\right\|^2\\ &> \frac{1}{2}\alpha^2\left\|\frac{\partial y_{O1}}{\partial \mathbf{W}}\right\|^2\left\|e_1(k)\frac{\partial y_{O1}}{\partial \mathbf{W}} + e_2(k)\frac{\partial y_{o2}}{\partial \mathbf{W}}\right\|^2 \cos^2\phi_1\\ &\quad + \frac{1}{2}\alpha^2\left\|\frac{\partial y_{O2}}{\partial \mathbf{W}}\right\|^2\left\|e_1(k)\frac{\partial y_{O1}}{\partial \mathbf{W}} + e_2(k)\frac{\partial y_{o2}}{\partial \mathbf{W}}\right\|^2 \cos^2\phi_2\end{aligned} \tag{49}$$

a true condition provided the following inequations are fulfilled:

$$\begin{aligned}2 &> \alpha\left\|\frac{\partial y_{O1}}{\partial \mathbf{W}}\right\|^2 + \alpha\left\|\frac{\partial y_{O2}}{\partial \mathbf{W}}\right\|^2\\ 0 &< \alpha < \frac{1}{\left\|\frac{\partial y_{Op}(k)}{\partial \mathbf{W}(k)}\right\|^2_{\max}}\end{aligned} \tag{50}$$

where the vector $\mathbf{W}$ is made up of all the coefficients adjusted in each sampling cycle.

This expression indicates a sufficient condition for ensuring the stability of the neural network adjustment

process with 2 outputs, adjusted by the gradient descent method.

Acknowledgments

The authors would like to express their grateful thanks of the work carried out by the members of the SIAMO project; without their help the practical wheelchair tests could not have been conducted.

References

Acosta, L., Méndez, J.A., Torres, S., Moreno, L., and Marichal, G.N. 1999. On the design and implementation of a neuromorphic selft-tuning controller. *Neural Processing Letters*, 9(3):229–242.

Boquete, L., Barea, R., García, R., Mazo, M., and Espinosa, F. 1999a. Identification and control of a wheelchair using recurrent neural networks. *Engineering Applications of Artificial Intelligence*, 12(4):443–452.

Boquete, L., García, R., Barea, R., and Mazo, M. 1999b. Neural control of the movements of a wheelchair. *Journal of Intelligent and Robotic Systems*, 25(3):213–226.

Boquete, L., Martín, P., Mazo, M., García, R., Barea, R., Rodríguez, F.J., and Fernández, I. 2002. Hardware implementation of a new neurocontrol wheelchair-guidance system. *Neurocomputing*, 47(1):145–160.

Brown, K.E., Iñigo, R.M., and Johnson, B.W. 1990. Design, implementation and testing of an adaptable optimal controller for an electric wheelchair. *IEEE Transactions on Industrial Applications*, 26(6):1144–1157.

Campolucci, P., Uncini, A., Piazza, F., and Rao, B.D. 1999. On-line learning algorithms for locally recurrent neural networks. *IEEE Transactions on Neural Networks*, 10(2):253–271.

Chen, C.-L., Chen, W.-C., and Chang, F.-Y. 1993. Hybrid learning algorithm for Gaussian potential function networks. *IEE Proceedings-d*, 140(6):442–448.

Ciocoiu, I.B. 1996. Radial base function networks with FIR/IIR synapses. *Neural Processing Letters*, 3:7–22.

Cooper, R.A. 1995. Intelligent control of power wheelchairs. *IEEE Engineering in Medicine and Biology*, 4:423–431.

Cooper, R.A., Corfman, T.A., Fitzgerald, S.G., Boninger, M.L., Spaeth, D.M., Ammer, W., and Arva, J. 2002. Perfomance assessment of a pushrim-activated power-assisted wheelchair control system. *IEEE Transactions on Control Systems Technology*, 10(1):121–126.

Elman, J.L. 1990. Finding structure in time. *Cognitive Sci.*, 14:179–211.

Espinosa, F., López, E., Mateos, R., Mazo, M., and García, R. 2001. Advanced and intelligent control techniques applied to the drive control and path tracking systems on a robotic wheelchair. *Autonomous Robots*, 11:137–148.

Figueiredo, R.J.P. 1998. Optimal interpolating and smoothing functional artificial neural networks (FANN'S) based on a generalized fock space framework. *Circuits Syst. Signal Processing*, 17:271–287.

Krovi, V. and Kumar, V. 1999. Modeling and control of a hybrid locomotion system. *ASME Journal of Mechanical Design*, 121(3):448–455.

Ku, C.C. and Lee, K.Y. 1995. Diagonal recurrent neural networks for dynamic systems control. *IEEE Transactions on Neural Networks*, 6(1):144–156.

Kuc, T.-Y., Baek, S.-M., and Park, K. 2001. Adaptive learning controller for autonomous mobile robots. *IEE Proc.-Control Theory Apply*, 148(1):49–54.

Maeda, Y. and Figueiredo, R. J. P. 1997. Learning rules for neurocontroller via simultaneous perturbation. *IEEE Transactions on Neural Networks*, 8(5):1119–1130.

Mazo, M. et al. 2001. An integral system for assisted mobility. *IEEE Robotics & Automation Magazine*, 7(1):46–56.

Mulgrew, B. 1996. Appliying radial basis functions. *IEEE Signal Processing Magazine*, 13(2):50–65.

Narendra, K.S. and Parthasarathy, K. 1990. Identification and control of dynamical systems using neural networks. *IEEE Transactions on Neural Networks*, 1(1):4–27.

Oriolo, G., de Luca, A., and Vendittelli, M. 2002. WMR control via dynamic feedback linearization: Design, implementation and experimental validation. *IEEE Transactions on Control Systems Technology*, 10(6):835–852.

Sastry, P.S., Santharam, G., and Unnikrishnan, K.P. 1994. Memory neuron networks for identification and control of dynamical systems. *IEEE Transactions on Neural Networks*, 5(2):306–319.

Tsoi, A.C. and Back, A.D. 1994. Locally recurrent globally feedforward networks: A critical review of architectures. *IEEE Transactions on Neural Networks*, 5(2):229–239.

Wellman, P., Krovi, V., Kumar, V., and Harwin, W. 1995. Design of a wheelchair with legs for people with motor disabilities. *IEEE Transactions on Rehabilitation Engineering*, 3(4):343–349.

Yu, H., Spenko, M., and Dubowsky, S. 2003. An adaptive shared control system for an intelligent mobility aid for the elderly. *Autonomous Robots*, 15:53–66.

Zhang, Y., Sen, P., and Hearn, G.E. 1995. An on-line trained adaptive neural controller. *IEEE Control Systems*, 15(5):67–75.

Luciano Boquete received a Ph.D. in Telecommunications in 1998, a degree in Telecommunications Engineering in 1994 and a degree in Technical Telecommunications Engineering in 1987. He is currently an Associate Professor in the Electronics Department at the Alcalá University (Spain). His research interests include bioengineering, computer vision, system control, and neural networks. He

is the author of more than 100 refereed publications in international journals, book chapters, and conference proceedings.

Rafael Barea received a Ph.D. degree in Telecommunications from University of Alcalá in 2001, a M.S. degree in Telecommunications from the Polytechnic University of Madrid in 1997 and a B.S. degree in Telecommunications Engineering with first Class Honours from the University of Alcalá in 1994. He has been a Lecturer in the Electronics Department at the University of Alcalá since 1994. His research interest include bioengineering, medical instrumentation, personal robotic aids, computer vision, system control, and neural networks. He is the author of numerous refereed publications in international journals, book chapters, and conference proceedings.

Ricardo García received a Ph.D. in Telecommunications in 1993, and a degree in Telecommunications Engineering from the Polytechnic University of Madrid in 1974. He has been a Lecturer in the Electronics Department at the University of Alcalá since 1975. His areas of research are systems control, optimal control, robust control, and neural networks.

Manuel Mazo received a Ph.D. degree in Telecomunications in 1988, and Engineering degree (M.S) in Telecomunications in 1982, all of them from the Polytechnic University of Madrid (Spain). Currently, he is a Professor at the Departament of Electronics, University of Alcalá. His areas of research are multi-sensor (ultrasonic, infrared and artificial vision) integration and electronic control systems applied to mobile robots and wheelchairs for physically disabled people. He has collaborated on several research projects in all these areas. He is the author of numerous refereed publications in international journals, book chapters, and conference proceedings. He is a IEEE member.

Miguel Ángel Sotelo received the Dr. Ing. degree in Electrical Engineering in 1996 from the Technical University of Madrid, and the Ph.D. degree in Electrical Engineering in 2001 from the University of Alcalá, Alcalá de Henares, Madrid, Spain. From 1993 to 1994 he has been a Researcher at the Department of Electronics, University of Alcalá, where he is currently an Associate Professor. His research interests include real-time computer vision and control systems for autonomous and assisted intelligent road vehicles. He has been recipient of the Best Research Award in the domain of Automotive and Vehicle Applications in Spain, in 2002. He received a Special Mention in the 5th 3M Foundation Awards in the category of Vehicle Security in 2003. He is the author of more than 60 refereed publications in international journals, book chapters, and conference proceedings. He is a IEEE member.